

# On the possibility of generating a 4-neutron resonance with a $T = 3/2$ isospin 3-neutron force

E. Hiyama

*Nishina Center for Accelerator-Based Science, RIKEN, Wako, 351-0198, Japan*

R. Lazauskas

*IPHC, IN2P3-CNRS/Universite Louis Pasteur BP 28, F-67037 Strasbourg Cedex 2, France*

J. Carbonell

*Institut de Physique Nucléaire, Université Paris-Sud, IN2P3-CNRS, 91406 Orsay Cedex, France*

M. Kamimura

*Department of Physics, Kyushu University, Fukuoka 812-8581, Japan and  
Nishina Center for Accelerator-Based Science, RIKEN, Wako 351-0198, Japan*

(Dated: September 26, 2018)

We consider the theoretical possibility to generate a narrow resonance in the four neutron system as suggested by a recent experimental result. To that end, a phenomenological  $T = 3/2$  three neutron force is introduced, in addition to a realistic  $NN$  interaction. We inquire what should be the strength of the  $3n$  force in order to generate such a resonance. The reliability of the three-neutron force in the  $T = 3/2$  channel is examined, by analyzing its consistency with the low-lying  $T = 1$  states of  ${}^4\text{H}$ ,  ${}^4\text{He}$  and  ${}^4\text{Li}$  and the  ${}^3\text{H} + n$  scattering. The *ab initio* solution of the  $4n$  Schrödinger equation is obtained using the complex scaling method with boundary conditions appropriate to the four-body resonances. We find that in order to generate narrow  $4n$  resonant states a remarkably attractive  $3N$  force in the  $T = 3/2$  channel is required.

## I. INTRODUCTION

The possibility of detecting a four-neutron ( $4n$ ) structure of any kind – bound or resonant state – has intrigued the nuclear physics community for the last fifty years (see Refs. [1–3] for historical reviews).

First of all, many experimental trials have been undertaken to seek for four-neutron systems, in particular some recurrent claims of such an observation have been published [4–8] but none of them has really been confirmed [9].

Theoretical studies were mostly concentrated in exploring the possible existence of bound multineutrons, agreeing in unison about the impossibility to observe a bound  $4n$  state [10–18]. None of the known nucleon-nucleon ( $NN$ ) interactions accommodate such a structure and the required modifications to ensure the  $4n$  binding – would they be at the  $2N$  or  $3N$  level – are so sizeable that the entire nuclear chart would be strongly perturbed. Several studies [14–16] indicate that the required additional extrabinding amounts to several tens of MeV, much beyond the uncertainties of current nuclear interaction models, including the  $3N$  forces

A different situation occurs for the  $4n$  resonant states. On the one hand, calculation of resonant states turns out to be a much more difficult task, both formally and technically. On the other hand, it is far from trivial to relate the calculated resonant state parameters, usually their  $S$ -matrix pole positions, to the experimental observables. Unless a resonant state is very narrow and, therefore, a Breit-Wigner parametrization is valid, the experimental observables have no straightforward relation with the  $S$ -matrix pole position of the resonance. In this case, a careful analysis of the reaction mechanism is necessary in order to establish a relation with the experimental observables. If a resonance is found very far from the real en-

ergy axis (physical domain) it will have no significant impact on a physical process.

Following this line of reasoning, some calculations based on semi-realistic  $NN$  forces indicated null [13] or unlikely evidence [14] for an observable  $4n$  resonance. On the other hand a Green's function Monte Carlo (GFMC) calculation [15] using the realistic AV18 [19]  $NN$  potential and Illinois-IL2  $3N$  forces [20] suggested a possible (broad) resonance at  $E_{R=2}$  MeV. This result was obtained by a linear extrapolation of tetra-neutrons binding energies, artificially bound in an external Woods-Saxon potential with  $V_0$  depth, in the limit  $V_0 \rightarrow 0$ . One should note, however, that in order to determine the position of a broad resonance by such a procedure, a special functional form must be used [21], which critically depends on the near threshold input values, an energy region where GFMC calculations are difficult to converge.

The *ab initio* solutions for the  $3n$  and  $4n$  states in the continuum were first presented in Refs. [17, 18] by solving the corresponding Faddeev-Yakubovsky (FY) equations [22] in the complex energy plane. The  $nn$ -interaction used was the charge dependent Reid-93 potential from the Nijmegen group [23]. In order to locate the resonance position of the physical tetra-neutron an *ad hoc*  $4n$  interaction was first added to the  $nn$  forces with the aim of artificially creating a  $4n$  bound state. The strength of this  $4n$  term was adiabatically decreased and the trajectory of the bound state singularity was traced in the complex energy plane from the negative real axis to the resonance position until it reached its physical point. The conclusion of this work was clear: none of the examined  $4n$  states ( $J^\pi = 0^\pm, 1^\pm, 2^\pm$ ) could manifest themselves as a near-threshold resonance. The corresponding pole trajectories moved too far from the real axis, reached the third energy quadrant and generated large widths  $\Gamma \sim 15$  MeV.

A recent experiment on the  ${}^4\text{He}({}^8\text{He}, {}^8\text{Be})4n$  reaction generated an excess of  $4n$  events with low energy in the final state. This observation has been associated with a possible  $4n$  resonance with an estimated energy  $E_R = 0.83 \pm 0.65 \pm 1.25$  MeV above the  $4n$  breakup threshold and an upper limit of width  $\Gamma = 2.6$  MeV [7, 8]. Low statistics, however, have not allowed one to extract the spin or parity for the corresponding state. It is worth noting that a further analysis of the experimental results of Ref. [4] concluded that the observed (very few) events were also compatible with a  $E_R = 0 - 2$  MeV tetra-neutron resonance [6].

In view of the obvious tension between the theoretical predictions and the last experimental results, we believe that it would be of some interest to reconsider this problem from a different point of view. In the dynamics of Ref. [17], the  $3n$  forces were not included, and the  $4n$  force added to the  $nn$  potential was a pure artifact for binding the system and controlled the singularity when moving into the resonance region in the complex energy plane.

The  $NN$  interaction models are almost perfect in the sense of  $\chi^2/\text{data} \approx 1$ . This was already the case with the Nijmegen [23], Bonn [24] and Argonne [19] charge symmetry breaking versions, despite some arbitrariness in their meson contents and couplings. The remarkable progress that the effective field theory (EFT) approach to nuclear physics offers, even though it does not dramatically improve the agreement between the  $NN$  models and  $NN$  data, does allow a high degree of consistency and refinement that leaves little room for improvement.

The  $nn$  interaction part is the least constrained due to the absence of the experimental data on  $nn$  scattering. Still, as observed in Ref. [16, 18], the margin of uncertainty to make the tetra-neutron bound or visibly resonant remains quite limited.

The two-neutron system is virtual state in the  ${}^1S_0$  partial wave but any arbitrary enhancement introduced to obtain the  $4n$  binding would be in conflict with the unbound – or loosely bound [25] – dineutron. However, due to the Pauli principle the effective interaction between dineutrons is mostly repulsive and this partial wave does not contribute much in building attraction between the dineutron pairs.

In contrast, the Pauli principle does not prevent  $P$ - and higher partial waves contributions from increasing the attraction between a dineutron and another neutron. Moreover  $P$ -waves have been a long standing controversy in nuclear physics [26–28], and some few-nucleon scattering observables (as analyzing powers) would favor stronger  $P$ -waves. Nevertheless the discrepancies with scattering data might be accounted for by a small variation of the  $nn$   $P$ -waves, of the order of 10%. In fact, some previous studies [16] showed that, in order to bind the tetra-neutron, the attractive  $nn$   $P$ -waves should be multiplied by a factor  $\eta \sim 4$ , rendering the dineutron strongly resonant in these  $P$ -waves. One should also notice that if all the  $nn$   $P$ -wave interactions are enhanced with the same factor  $\eta$ , the dineutron becomes bound well before the tetra-neutron. In order to create a narrow  $4n$  resonance, a slightly weaker enhancement is required, but still this enhancement factor remains considerable,  $\eta \gtrsim 3$ . Therefore such a modification strongly contradicts the nature of the nu-

clear interaction, which satisfies rather well isospin conservation.

Finally, as noted in Ref. [20], a three-neutron force might make a key contribution in building the additional attraction required to generate resonant multineutron clusters. As we will see in the next section, the presence of an attractive  $T = 3/2$  component in the  $3N$  force is clearly suggested in the studies based on the best  $NN$  and  $T = 1/2$   $3N$  potentials, which often underestimate the binding energies of the neutron-rich systems. Furthermore the contribution of such a force should rise quickly with the number of neutrons in the system, and we will indeed demonstrate this when comparing  $3n$  and  $4n$  systems.

In our previous studies [16, 18] we have employed different realistic  $NN$  interaction models (Reid93, AV18, AV8', INOY) in analyzing multineutron systems and found that they provide qualitatively the same results. For all these reasons we will focus on the modification of the  $3N$  force in the total isospin  $T = 3/2$  channel. The main purpose of this work is, thus, to investigate whether a resonant tetra-neutron state is compatible with our knowledge of the nuclear interaction, in particular with the  $T = 3/2$   $3N$  force. To this aim we will fix the  $NN$  force with a realistic interaction and introduce a simple isospin-dependent  $3N$  force acting in both isospin channels. Its  $T = 1/2$  part will be adjusted to describe some  $A = 3$  and  $A = 4$  nuclear states and the  $T = 3/2$  part will be tuned until a  ${}^4n$  resonance is manifested. The exploratory character of this study, as well as the final conclusions, justify the simplicity of the phenomenological force adopted here.

The paper is organized as follows. In Section II we will present the  $NN$  and  $3N$  interactions and the unique adjustable parameter of the problem. Section III is devoted to sketching the complex scaling method [29–33] that is used to solve the  $4n$  Schrödinger equation under the correct boundary condition for resonant states. Also we briefly explain the Gaussian expansion method [34–39] and the FY equations for solving the  $A = 4$  problem. Results obtained are presented and discussed in the Section IV; finally conclusions are drawn in the last Section V.

## II. HAMILTONIAN

We start with a general nonrelativistic nuclear Hamiltonian

$$H = T + \sum_{i<j} V_{ij}^{NN} + \sum_{i<j<k} V_{ijk}^{3N}, \quad (2.1)$$

where  $T$  is a four-particle kinetic-energy operator,  $V_{ij}^{NN}$  and  $V_{ijk}^{3N}$  are respectively two- and three-nucleon potentials. In this work we use the AV8' version [40] of the  $NN$  potentials derived by the Argonne group. This model describes well the main properties of the  $NN$  system and it is relatively easy to handle. The main properties of this interaction are outlined in the benchmark calculation of the  ${}^4\text{He}$  ground state [41].

As most  $NN$  forces, AV8' fails to reproduce binding energies of the lightest nuclei, in particular those of  ${}^3\text{H}$ ,  ${}^3\text{He}$  and

${}^4\text{He}$ . A  $3N$  interaction is required and we have therefore supplemented AV8' with a purely phenomenological  $3N$  force which is assumed to be isospin-dependent and given by a sum of two Gaussian terms:

$$V_{ijk}^{3N} = \sum_{T=1/2}^{3/2} \sum_{n=1}^2 W_n(T) e^{-(r_{ij}^2 + r_{jk}^2 + r_{ki}^2)/b_n^2} \mathcal{P}_{ijk}(T). \quad (2.2)$$

where  $\mathcal{P}_{ijk}(T)$  is a projection operator for the total three-nucleon isospin  $T$  state. The parameters of this force – its strength  $W_n$  and range  $b_n$  – are adjusted to reproduce the phenomenology.

In the case of  $T = 1/2$  the parameters were fixed in Ref. [42] when studying the  $J^\pi = 0^+$  states of  ${}^4\text{He}$  nucleus. They are:

$$\begin{aligned} W_1(T = 1/2) &= -2.04 \text{ MeV}, & b_1 &= 4.0 \text{ fm}, \\ W_2(T = 1/2) &= +35.0 \text{ MeV}, & b_2 &= 0.75 \text{ fm}. \end{aligned} \quad (2.3)$$

Using this parameter set, in addition to the AV8' and Coulomb interaction, one obtains the following binding energies:  ${}^3\text{H}=8.41$  (8.48) MeV,  ${}^3\text{He}=7.74$  (7.72) MeV,  ${}^4\text{He}(0_1^+)=28.44$  (28.30) MeV and the excitation energy of  ${}^4\text{He}(0_2^+)=20.25$  (20.21) MeV [42], where the experimental values are shown in parentheses. Furthermore, this parameterization allows one to reproduce the observed transition form factor  ${}^4\text{He}(e, e'){}^4\text{He}(0_2^+)$  (cf. Fig. 3 of Ref. [42]).

Although the  ${}^3\text{H}$  and  ${}^3\text{He}$  nuclei contain in their wave functions a small admixture of isospin  $T = 3/2$  configurations, these calculations have been performed by neglecting it, as it is the case in most of the few-nucleon calculations.

The  $4n$  system is only sensitive to the  $T = 3/2$  component of the  $3N$  interaction. This component has almost no effect in proton-neutron symmetric nuclei, but it manifests clearly itself in the series of He isotopes, where the purely  $T = 1/2$

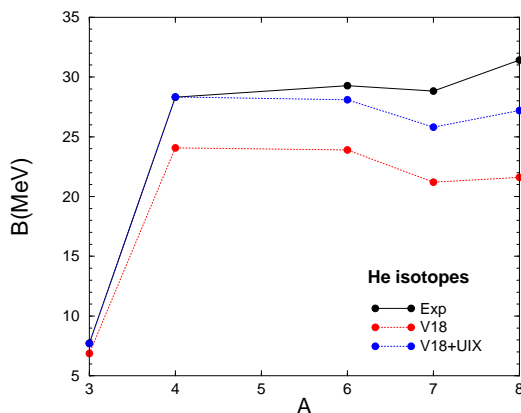


FIG. 1: (color online) Experimental binding energies of the He isotopes compared with the predictions based on AV18 and AV18+UIX Hamiltonians. The UIX  $3N$  force is purely repulsive in the  $T = 3/2$  channel and exhibits attraction only in the  $T = 1/2$  one. Displayed values are taken from Table II of Ref. [20].

$3N$  force, adjusted to reproduce well the  ${}^4\text{He}$ , fails to describe the increasingly neutron-rich He isotopes. This can be illustrated with the results of the GFMC calculations, Table II of Ref. [20], which are displayed in Fig. 1.

This situation was dramatically improved in Ref. [20], where several  $3 \leq A \leq 8$  nuclei were used to fix the parameters of a new series of spin-isospin dependent Illinois  $3N$  forces (IL1–IL5) which reproduce well the experimental data in Fig. 1. It is worth noting however that, from the results in Fig. 1, the effect of the  $T = 3/2$  component of the  $3N$  force remains smaller than the  $T = 1/2$  component.

Throughout the present paper, the attractive strength parameter of the  $T = 3/2$  component,  $W_1(T = 3/2)$ , will be considered as a free parameter and varied in order to analyze the existence of a possible tetra-neutron resonance. The other parameters retain the same value as in the  $T = 1/2$  case; that is we use:

$$\begin{aligned} W_1(T = 3/2) &= \text{free}, & b_1 &= 4.0 \text{ fm}, \\ W_2(T = 3/2) &= +35.0 \text{ MeV}, & b_2 &= 0.75 \text{ fm}. \end{aligned} \quad (2.4)$$

We will explore in parallel the effect of such a force on the  $A = 4$  nuclei that could be sensitive to the  $T = 3/2$  component, that is:  ${}^4\text{H}$ ,  ${}^4\text{He}$  and  ${}^4\text{Li}$ , in states with total isospin  $T = 1$  and angular momentum  $J^\pi = 1^-$  and  $2^-$ .

### III. COMPUTATIONAL METHOD

Two independent configuration space methods are used in solving the four-body problem: the Gaussian expansion method [34–39] is applied to solve Schrödinger equation and Lagrange-mesh technique applied to solve FY equation. In order to simplify boundary conditions related to the four-body problem in the continuum we employ the complex scaling method [29–33]. These methods will be briefly sketched in what follows.

#### A. Complex scaling Method

In this work, we focus on the possible existence of the narrow resonant states of  ${}^4n$ , which may enhance significantly  ${}^4n$  production cross section. We employ the complex scaling method (CSM) in order to calculate resonance positions and widths. The CSM and its application to nuclear physics problems are extensively reviewed in Refs. [43, 44] and references therein. Using the CSM, the resonance energy (its position and width) is obtained as a stable complex eigenvalue of the complex scaled Schrödinger equation:

$$[H(\theta) - E(\theta)]\Psi_{JM,TT_z}(\theta) = 0, \quad (3.1)$$

where  $H(\theta)$  is obtained by making the radial transformation of the four-body Jacobi coordinates (Fig. 1) in  $H$  of Eq. (2.1) with respect to the common complex scaling angle of  $\theta$ :

$$r_c \rightarrow r_c e^{i\theta}, \quad R_c \rightarrow R_c e^{i\theta}, \quad \rho_c \rightarrow \rho_c e^{i\theta} \quad (c = K, H). \quad (3.2)$$

According to the ABC theorem [29, 30], the eigenvalues of Eq. (3.1) may be separated into three groups:

i) The bound state poles, remain unchanged under the complex scaling transformation and remain on the negative real axis.

ii) The cuts, associated with discretized continuum states, are rotated downward making an angle of  $2\theta$  with the real axis.

iii) The resonant poles are independent of parameter  $\theta$  and are isolated from the discretized non-resonant continuum spectrum lying along the  $2\theta$ -rotated line when the relation  $\tan 2\theta > -\text{Im}(E_{\text{res}})/\text{Re}(E_{\text{res}})$  is satisfied. The resonance width is defined by  $\Gamma = -2 \text{Im}(E_{\text{res}})$ .

In the next subsection, we shall show, as an example satisfying the above properties i)-iii), narrow and broad  $^4n$  resonances and the  $4n$  continuum spectrum rotated into the complex energy plane.

### B. Gaussian expansion method

A great advantage of the CSM is that it allows one to describe the resonant states using  $L^2$ -integrable wave functions. Therefore, the Gaussian expansion method (GEM) [34–39] has been successfully applied in conjunction with the CSM in nuclear few-body calculations [43–45] as well as in recent three- and four-body calculations by two authors (E.H. and M.K.) of the present manuscript [46–48].

In order to expand the system's wave function  $\Psi_{JM,TT_z}(\theta)$  we employ the Gaussian basis functions of the same type as those used in the aforementioned references. An isospin rather than a neutron-proton (particle) basis is used to distinguish between different nuclear charge states  $^4n$ ,  $^4\text{H}$ ,  $^4\text{He}$  and  $^4\text{Li}$ . In the GEM approach, the four-nucleon wave function is written as a sum of the component functions in the K- and H-type Jacobi coordinates (Fig. 2), employing the  $LS$  coupling scheme:

$$\Psi_{JM,TT_z}(\theta) = \sum_{\alpha} C_{\alpha}^{(\text{K})}(\theta) \Phi_{\alpha}^{(\text{K})} + \sum_{\alpha} C_{\alpha}^{(\text{H})}(\theta) \Phi_{\alpha}^{(\text{H})}, \quad (3.3)$$

where the antisymmetrized four-body basis functions  $\Phi_{\alpha}^{(\text{K})}$  and  $\Phi_{\alpha}^{(\text{H})}$  (whose suffix  $JM, TT_z$  are dropped for simplicity) are described by

$$\begin{aligned} \Phi_{\alpha}^{(\text{K})} = \mathcal{A} \left\{ \left[ \left[ \left[ \phi_{nl}^{(\text{K})}(\mathbf{r}_{\text{K}}) \varphi_{\nu\lambda}^{(\text{K})}(\boldsymbol{\rho}_{\text{K}}) \right]_{\Lambda} \psi_{NL}^{(\text{K})}(\mathbf{R}_{\text{K}}) \right]_I \right. \right. \\ \times \left. \left[ \chi_s(12) \chi_{1/2}(3) \right]_{s'} \chi_{1/2}(4) \right]_S \Big]_{JM} \\ \times \left. \left[ \eta_t(12) \eta_{1/2}(3) \right]_{t'} \eta_{1/2}(4) \right]_{TT_z} \Big\}, \quad (3.4) \end{aligned}$$

$$\begin{aligned} \Phi_{\alpha}^{(\text{H})} = \mathcal{A} \left\{ \left[ \left[ \left[ \phi_{nl}^{(\text{H})}(\mathbf{r}_{\text{H}}) \varphi_{\nu\lambda}^{(\text{H})}(\boldsymbol{\rho}_{\text{H}}) \right]_{\Lambda} \psi_{NL}^{(\text{H})}(\mathbf{R}_{\text{H}}) \right]_I \right. \right. \\ \times \left. \left[ \chi_s(12) \chi_{s'}(34) \right]_S \right]_{JM} \\ \times \left. \left[ \eta_t(12) \eta_{t'}(34) \right]_{TT_z} \right\}, \quad (3.5) \end{aligned}$$

with  $\alpha \equiv \{nl, \nu\lambda, \Lambda, NL, I, s, s', S, t, t'\}$ .  $\mathcal{A}$  is the four-nucleon antisymmetrizer. The parity of the wave function is

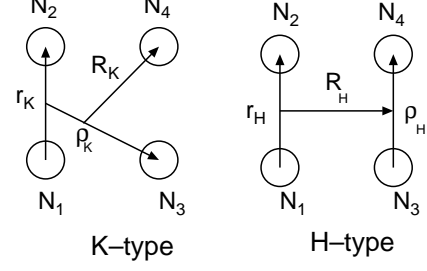


FIG. 2: Four-nucleon Jacobi coordinates of K-type and H-type configurations. .

given by  $\pi = (-)^{l+\lambda+L}$ . The  $\chi$ 's and  $\eta$ 's are the spin and isospin functions, respectively. The spatial basis functions  $\phi_{nl}(\mathbf{r})$ ,  $\varphi_{\nu\lambda}(\boldsymbol{\rho})$  and  $\psi_{NL}(\mathbf{R})$  are taken to be Gaussians multiplied by spherical harmonics:

$$\begin{aligned} \phi_{nlm}(\mathbf{r}) &= N_{nl} r^l e^{-(r/r_n)^2} Y_{lm}(\hat{\mathbf{r}}), \\ \varphi_{\nu\lambda\mu}(\boldsymbol{\rho}) &= N_{\nu\lambda} \rho^\lambda e^{-(\rho/\rho_\nu)^2} Y_{\lambda\mu}(\hat{\boldsymbol{\rho}}), \\ \psi_{NLM}(\mathbf{R}) &= N_{NL} R^L e^{-(R/R_N)^2} Y_{LM}(\hat{\mathbf{R}}). \end{aligned} \quad (3.6)$$

It is important to postulate that the Gaussian ranges lie in geometric progression (for the reason, see Sec. IIB of the first paper of Ref. [39]):

$$\begin{aligned} r_n &= r_1 a^{n-1} & (n = 1 - n_{\text{max}}), \\ \rho_\nu &= \rho_1 \alpha^{\nu-1} & (\nu = 1 - \nu_{\text{max}}), \\ R_N &= R_1 A^{N-1} & (N = 1 - N_{\text{max}}). \end{aligned} \quad (3.7)$$

Such a choice of basis functions is suitable for simultaneous description of short-range correlations and long-range asymptotic behavior (for example, see Refs. [34–39, 46]).

The eigenenergy  $E(\theta)$  and the expansion coefficients in Eq. (3.3) are obtained by diagonalizing the Hamiltonian  $H(\theta)$  with the basis functions (3.4) and (3.5). In the following calculations, satisfactory convergence was obtained within  $l, L, \lambda \leq 2$  (cf. an example of rapid convergence in the binding energies of  $^3\text{H}$  and  $^3\text{He}$  with realistic  $NN$  and  $3N$  interactions is presented in Refs. [35, 36]). We note that, in the GEM framework, contrary to the truncation in the wave function, the interaction is included without partial-wave decomposition (no truncation in the angular-momentum space); this makes the convergence rapid (cf. discussion on this point in §2.2 of Ref. [49]).

In Fig. 3 we present two typical applications of the GEM in diagonalizing the complex-scaled Hamiltonian  $H(\theta)$  that describes the  $^4n$  system. The two panels of this figure display the  $\theta$ -dependence of the eigenenergies for the cases where the  $^4n$  system possesses a) a narrow resonance and b) a broad resonance with  $\Gamma = -2 \text{Im}(E_{\text{res}}) \sim 6$  MeV. The resonance pole position converges when increasing the complex scaling angle  $\theta$ , and the pole becomes well isolated from the four-body continuum along the  $2\theta$ -line. To obtain the result in Fig. 3, some 14000 antisymmetrized four-body basis functions were needed.

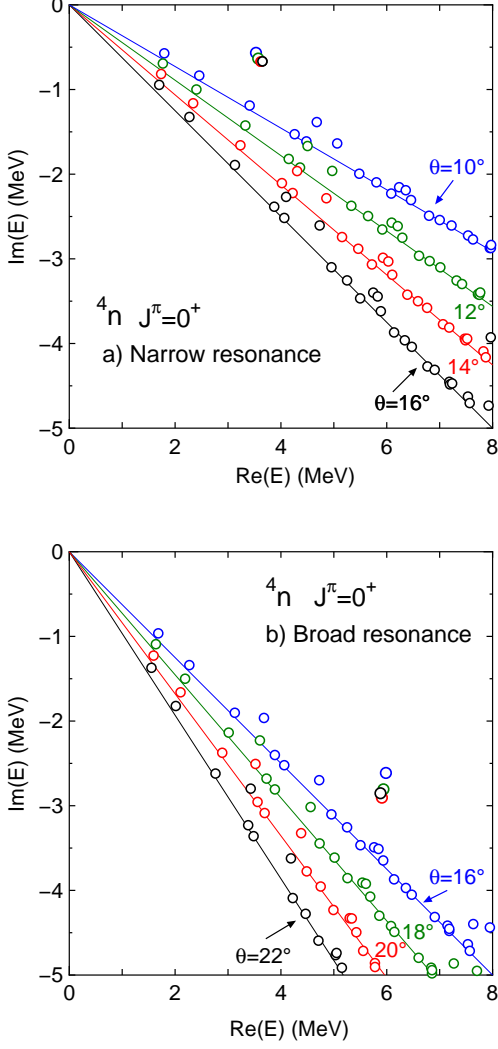


FIG. 3: (color online) Dependence of the eigenenergy distribution on the complex scaling angle  $\theta$  for the  ${}^4n$  system with  $J^\pi = 0^+$ . Two different cases are considered a) presence of a narrow resonance at  $E_{\text{res}} = 3.65 - 0.66i$  MeV for  $W_1(T = 3/2) = -28$  MeV and b) presence of a broad resonance at  $E_{\text{res}} = 5.88 - 2.85i$  MeV for  $W_1(T = 3/2) = -21$  MeV.

### C. Faddeev-Yakubovsky equations

The FY equations use a very similar representation of the system's wave function as the one employed by the GEM and presented in a previous section. The FY equations are formulated in terms of wave function components, which are very similar to the ones expressed in Eqs. (3.4) and (3.5), namely:

$$\begin{aligned} \mathcal{F}_\alpha^{(K)} = & \sum_{\alpha_K} C_{\alpha_K} \left[ [ [\phi_{nl}^{(K)}(\mathbf{r}_K) \varphi_{\nu\lambda}^{(K)}(\boldsymbol{\rho}_K)]_\Lambda \psi_{NL}^{(K)}(\mathbf{R}_K) ]_I \right. \\ & \times [ [\chi_s(12) \chi_{1/2}(3)]_{s'} \chi_{1/2}(4) ]_S ]_{JM} \\ & \times [ [\eta_t(12) \eta_{1/2}(3)]_{t'} \eta_{1/2}(4) ]_{TT_z}, \end{aligned} \quad (3.8)$$

$$\begin{aligned} \mathcal{F}_\alpha^{(H)} = & \sum_{\alpha_H} C_{\alpha_H} \left[ [ [\phi_{nl}^{(H)}(\mathbf{r}_H) \varphi_{\nu\lambda}^{(H)}(\boldsymbol{\rho}_H)]_\Lambda \psi_{NL}^{(H)}(\mathbf{R}_H) ]_I \right. \\ & \times [ \chi_s(12) \chi_{s'}(34) ]_S ]_{JM} [ \eta_t(12) \eta_{t'}(34) ]_{TT_z}. \end{aligned} \quad (3.9)$$

The major difference in the expansions of Eqs. (3.4) and (3.5) employed for the GEM is that the FY components are not straightforwardly antisymmetrized. Symmetry of the total wave function is enforced by the FY equations whose components are subject to, namely:

$$\begin{aligned} (E - H_0 - V_{12}) \mathcal{F}_\alpha^{(K)} - V_{12}(P^+ + P^-) [(1 + Q)\mathcal{F}_\alpha^{(K)} + \mathcal{F}_\alpha^{(H)}] \\ = \frac{1}{3} V_{123} \Psi_{JM, TT_z}, \end{aligned}$$

$$(E - H_0 - V_{12}) \mathcal{F}_\alpha^{(H)} - V_{12} \tilde{P} [(1 + Q)\mathcal{F}_\alpha^{(K)} + \mathcal{F}_\alpha^{(H)}] = 0,$$

where  $P^- = P_{23}P_{12}$ ,  $P^+ = P_{12}P_{23}$ ,  $Q = P_{34}$  and  $\tilde{P} = P_{13}P_{24}$  are particle permutation operators.

In terms of the FY components the total system wave function is obtained as

$$\begin{aligned} \Psi_{JM, TT_z}(\theta) = & \sum_{\alpha} [1 + (1 + P^+ + P^-)Q] (1 + P^+ + P^-) \mathcal{F}_\alpha^{(K)} \\ & + \sum_{\alpha} (1 + P^+ + P^-) \tilde{P} \mathcal{F}_\alpha^{(H)}. \end{aligned} \quad (3.10)$$

It is straightforward to apply the complex scaling operation to the FY equations, as has been demonstrated for the Schrödinger Eq. (3.1). For a more detailed explanation see one of our previous papers [17, 45].

The transformed FY equations are solved using standard techniques, developed in [16, 17] and references therein. The radial dependence of the complex-scaled FY components  $\mathcal{F}_\alpha^{(K)}$  and  $\mathcal{F}_\alpha^{(H)}$  is expanded in a Lagrange-Laguerre basis and the system of integro-differential equations is transformed into a linear algebra problem by using the Lagrange-mesh method [50]. Lagrange-mesh of  $\sim (20 - 25)^3$  points is required to describe accurately the radial dependence of the FY components. The FY equations converge considerably slower in partial-waves compared to the Schrödinger equation case using the GEM. When solving the FY equations we include partial-waves with angular momenta  $\max(l, L, \lambda) \leq 7$ . Slow convergence of these calculations is related to the  $3N$  force terms we employed in this work, whose contribution turns out to be unnaturally large. The FY equations are not very well formulated to handle these terms.

## IV. RESULTS AND DISCUSSION

The recent experiment, providing evidence of the possible existence of a resonant tetraneutron, reported some structure at  $E = 0.83 \pm 0.65(\text{stat.}) \pm 1.25(\text{sys.})$  MeV, measured with respect to the  $4n$  breakup threshold with an estimated upper limit width  $\Gamma = 2.6$  MeV [7, 8]. This experiment, as well as others reporting a positive tetraneutron signal [4–6] were not able to extract information on the spin-parity of the observed events. Our first task is therefore to determine the most favorable angular momentum states to accommodate a tetraneutron.

### A. $4n$ bound state

For this purpose, we calculate a critical strength of the attractive  $3N$  force  $W_1(T = 3/2)$ , defined by Eq. (2.2), to make different  $4n$  states bound at  $E = -1.07$  MeV. This energy corresponds to the lowest value compatible with the RIKEN data [8]. The calculated results, denoted as  $W_1^{(0)}(T = 3/2)$ , are given in Table I.

TABLE I: Critical strength  $W_1^{(0)}(T = 3/2)$  (MeV) of the phenomenological  $T = 3/2$   $3N$  force required to bind the  $4n$  system at  $E = -1.07$  MeV, the lower bound of the experimental value [8], for different states as well as the probability (%) of their four-body partial waves.

$J^\pi$	$0^+$	$1^+$	$2^+$	$0^-$	$1^-$	$2^-$
$W_1^{(0)}(T = \frac{3}{2})$	-36.14	-45.33	-38.05	-64.37	-61.74	-58.37
<i>S</i> -wave	93.8	0.42	0.04	0.07	0.08	0.08
<i>P</i> -wave	5.84	98.4	17.7	99.6	97.8	89.9
<i>D</i> -wave	0.30	1.08	82.1	0.33	2.07	9.23
<i>F</i> -wave	0.0	0.05	0.07	0.0	0.10	0.74

As one can see from this table, the smallest critical strength is  $W_1^{(0)}(T = 3/2) = -36.14$  MeV and corresponds to the  $J = 0^+$  state. It is consistent with a result reported in Ref. [17], where the tetra-neutron binding was forced using an artificial four-body force in conjunction with the Reid93  $nn$  potential. The next most favorable configuration is established to be a  $2^+$  state, which is bound by 1.07 MeV for a  $3NF$  strength of  $W_1^{(0)}(T = 3/2)$ . The calculated level ordering is  $J^\pi = 0^+, 2^+, 1^+, 2^-, 1^-, 0^-$ . The level ordering calculated in Ref. [17] is  $J^\pi = 0^+, 1^+, 1^-, 2^-, 0^-, 2^+$ . These differences are related to the different binding mechanism of the four-nucleon force used in Ref. [17].

It should be noted that, in comparison with  $W_1(T = 1/2) = -2.04$  MeV established for the  $T = 1/2$   $3N$  force, we need extremely strong  $T = 3/2$  attractive term to make the  $4n$  system weakly bound; when the  $J = 0^+$  state is at  $E = -1.07$  MeV with  $W_1(T = 3/2) = -36.14$  MeV, the expectation values of the kinetic energy,  $NN$  and  $3N$  forces are  $+67.0, -38.6$  and  $-29.5$  MeV, respectively. We see that the expectation value of the  $3N$  potential is almost as large as that of  $NN$  potential. The validity of this strongly attractive  $T = 3/2$   $3N$  force will be discussed after presenting results for  $4n$  resonant states.

### B. $4n$ resonances

After determining critical strength of  $W_1(T = 3/2)$  required to bind the tetra-neutron we gradually release this parameter letting the  $4n$  system to move into the continuum. In

this way we follow complex-energy trajectory of the  $4n$  resonances for  $J = 0^+, 2^+$  and  $2^-$  states. We remind the readers that these trajectories are controlled by a single parameter  $W_1(T = 3/2)$ , whereas other parameters remain fixed at the values given in Eq.(2.3) and Eq.(2.4).

In Fig. 4a, we display the  $4n$  S-matrix pole (resonance) trajectory for  $J = 0^+$  state by reducing the strength parameter from  $W_1(T = 3/2) = -37$  to  $-16$  MeV in step of 1 MeV.

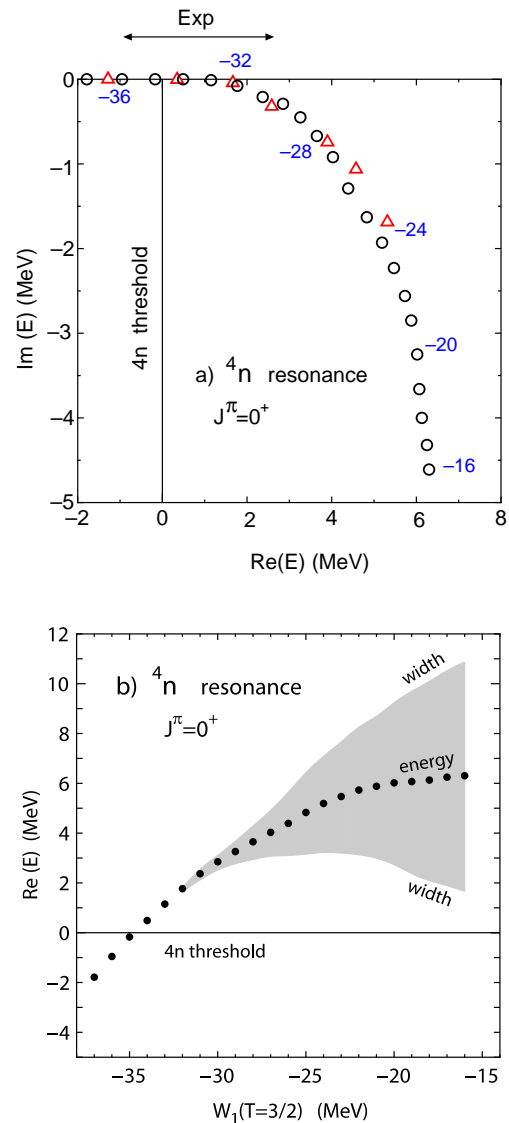


FIG. 4: a) Tetraneutron resonance trajectory for the  $J^\pi = 0^+$  state. The circles correspond to resonance positions for the AV8' and the triangles INOY04' (is-m) potential [28]. Parameter  $W_1(T = 3/2)$  of the additional  $3NF$  was changed from  $-37$  to  $-16$  MeV in steps of 1 MeV for calculations based on AV8' and from  $-36$  to  $-24$  MeV in steps of 2 MeV for INOY04' (is-m). To guide the eye the resonance region suggested by the measurement [8] is indicated by the arrow at the top. b) The same contents as in the upper panel figure (AV8'), but where the resonance energy (closed circles) and width (shaded area) are represented as a function of the  $W_1(T = 3/2)$  parameter.

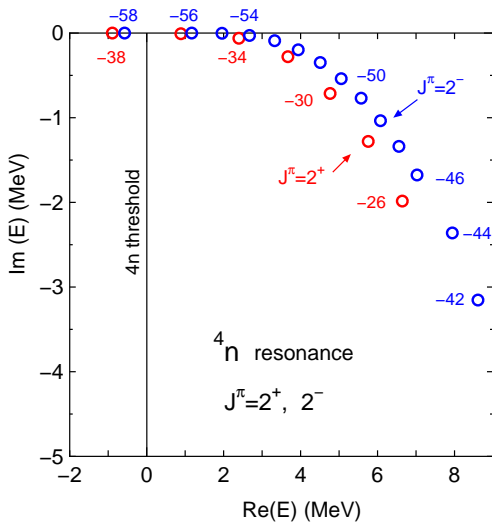


FIG. 5: (Color online) Tetra-neutron resonance trajectories for  $J^\pi = 2^+$  and  $2^-$  states for  $W_1(T = 3/2)$  values from  $-38$  to  $-26$  MeV and from  $-58$  to  $-42$  MeV, respectively.

We were unable to continue the resonance trajectory beyond the  $W_1(T = 3/2) = -16$  MeV value with the CSM, the resonance becoming too broad to be separated from the non-resonant continuum. To guide the eye, at the top of the same figure, we presented an arrow to indicate the  ${}^4n$  real energy range suggested by the recent measurement [8]. In that range the maximum value of the calculated decay width  $\Gamma$  is 0.6 MeV, which is to be compared with the observed upper limit width  $\Gamma = 2.6$  MeV. In Fig. 4b the contents of Fig. 4a are illustrated in a different manner to display explicitly the resonance energy and width versus  $W_1(T = 3/2)$ . The real energy of the resonances reaches its maximum value of  $\text{Re}(E_{\text{res}}) \sim 6$  MeV. Once its real energy maximum is reached the width starts quickly increasing as the strength  $W_1(T = 3/2)$  is further reduced.

As was expected, based on our experience from previous studies on multineutron systems [16, 18], tetra-neutron trajectory turns out to be independent of the  $NN$  interaction model, provided this model reproduces well the  $NN$  scattering data. To illustrate this feature we have calculated the  ${}^4n$  resonance trajectory for  $J = 0^+$  state using the INOY04(is-m)  $NN$  model [28]. This realistic interaction strongly differs from the other ones in that it contains a fully phenomenological and a strongly non-local short range part in addition to the typical local long range part based on one pion-exchange. Furthermore, this model reproduce the triton and alpha-particle binding energies without any 3NF contribution. Finally,  $P$ -waves of this interaction are slightly modified in order to match better the low energy scattering observables in the  $3N$  system. Regardless of the mentioned qualitative differences of the INOY04(is-m) interaction with respect to the AV8' one, the results for the  ${}^4n$  resonance trajectory are qualitatively the same and demonstrate only minor quantitative differences.

These results are displayed in Fig. 4a.

In Fig. 5, we present calculated  ${}^4n$  resonance trajectories for  $2^+$  and  $2^-$  states. The  $J = 2^+$  state is the next most favorable configuration to accommodate a bound tetra-neutron, whereas  $J = 2^-$  state is the most favorable negative parity state; see Table I. The trajectory of the  $2^+$  state is very similar to that of the  $0^+$  state. On the other hand in order to bind or even to produce a resonant  $J = 2^-$  state, in the region relevant for a physical observation, the attractive three-nucleon force term  $W_1(T = 3/2)$  should be almost twice as large as the one for  $J = 0^+$  state. The strength of  $W_1(T = 3/2)$  required to produce a resonant  ${}^4n$  system in any configuration producing a pronounced experimental signal, is one order of magnitude larger than the value of  $W_1(T = 1/2)$  ( $-2.04$  MeV) required to reproduce the binding energies of  ${}^3\text{H}$ ,  ${}^3\text{He}$  and  ${}^4\text{He}$  nuclei.

In order to prove or disprove the possible existence of the tetra-neutron resonances, one should consider the validity of the strongly attractive  $3N$  force in the isospin  $T = 3/2$  channel.

As pointed out in Sec. II, the GFMC calculation for  $3 \leq A \leq 8$  suggested the existence a 3NF with a  $T = 3/2$  component weaker than the  $T = 1/2$  one. From the same study it follows that the binding energies of neutron-rich nuclei are described without notable contribution of the  $T = 3/2$  channel in 3NF. A similar conclusion was reached in neutron matter calculations, where the expectation values of the  $T = 3/2$  force are always smaller than the  $T = 1/2$  ones [51]. One should mention that the parametrization of the phenomenological 3NF adapted in this study is very appropriate for dilute states, like the expected tetra-neutron resonances. The attractive 3NF term has a larger range than the one allowed by pion-exchange. Moreover tetra-neutron states, unlike compound  ${}^4\text{He}$  or  ${}^3\text{H}$  ground states, do not feel contributions of the short-ranged repulsive term of the  $3N$  force.

Thus, we find no physical justification for the fact that the  $T = 3/2$  term should be one order of magnitude more attractive than the  $T = 1/2$  one, as is required to generate tetra-neutron states compatible with the ones claimed in the recent experimental data [8].

### C. $T=1$ states in ${}^4\text{H}$ , ${}^4\text{He}$ and ${}^4\text{Li}$

In the following we would like to investigate the consequences of a strongly attractive 3NF component in the isospin

TABLE II: Observed energies  $E_R$  and widths  $\Gamma$  (in MeV) of the  $J^\pi = 2^-$  and  $1^-$  states in  ${}^4\text{H}$ ,  ${}^4\text{He}$  ( $T = 1$ ) and  ${}^4\text{Li}$ ,  $E_R$  being measured from the  ${}^3\text{H}+n$ ,  ${}^3\text{H}+p$  and  ${}^3\text{He}+p$  thresholds, respectively [52].

$J^\pi$	${}^4\text{H}$	${}^4\text{He}$ ( $T = 1$ )	${}^4\text{Li}$
	$E_R$ ( $\Gamma$ )	$E_R$ ( $\Gamma$ )	$E_R$ ( $\Gamma$ )
$2^-$	3.19 (5.42)	3.52 (5.01)	4.07 (6.03)
$1^-$	3.50 (6.73)	3.83 (6.20)	4.39 (7.35)

$T = 3/2$  channel. It is clear that such a force will have the most dramatic effect on nuclei with a large isospin number, i.e. neutron (or proton) rich ones as well as on infinite neutron matter. Nevertheless this includes mostly nuclei with  $A > 4$ , not within our current scope. Still we will investigate the effect on other well known states of  $A = 4$  nuclei, namely negative parity, isospin  $T = 1$  states of  ${}^4\text{H}$ ,  ${}^4\text{He}$  and  ${}^4\text{Li}$ . These structures represent broad resonances [52] (see Table II) established in nuclear collision experiments. Calculated energies of those states are shown in Fig. 6 with respect to increasing  $W_1(T = 3/2)$  from  $-37$  to  $0$  MeV. The solid curve below the corresponding threshold indicates a bound state, whereas

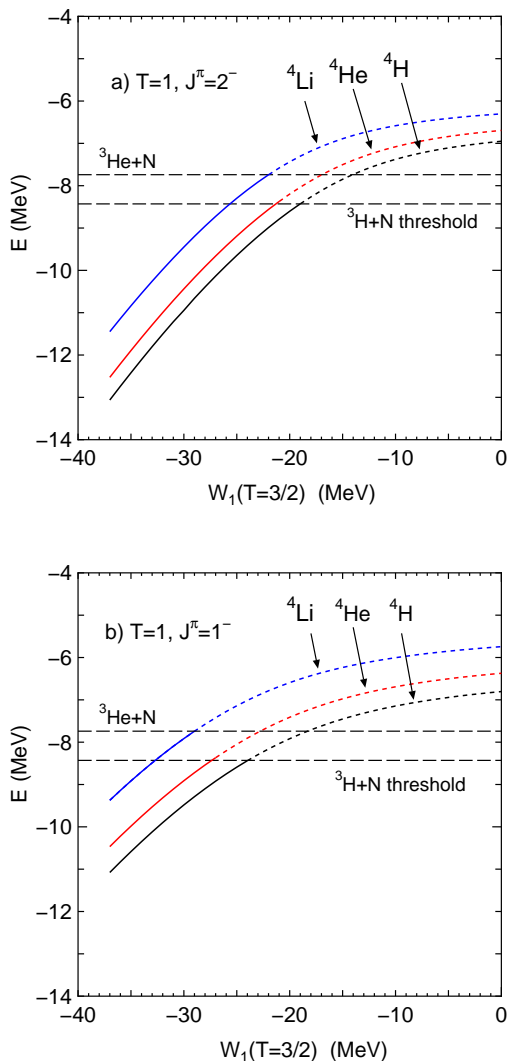


FIG. 6: (color online) a) Calculated energies of the lowest  $T = 1, J^\pi = 2^-$  states in  ${}^4\text{H}$ ,  ${}^4\text{He}$  and  ${}^4\text{Li}$  with respect to the strength of  $T = 3/2$  3N force,  $W_1(T = 3/2)$ . b) The same but for  $T = 1, J^\pi = 1^-$  states. The horizontal dashed lines show the  ${}^3\text{He} + N$  and  ${}^3\text{H} + N$  thresholds. The solid curve below the corresponding threshold indicates the bound state, while the dotted curve above the threshold stands approximately for the resonance obtained by the diagonalization of  $H(\theta = 0)$  with the  $L^2$  basis functions.

the dotted curve above the threshold stands approximately for the resonant state obtained within a bound state approximation, that is, by diagonalizing  $H(\theta = 0)$  with the  $L^2$  basis functions (3.4) and (3.5).

As demonstrated in Fig. 6, values of an attractive 3NF term in the range of  $W_1(T = 3/2) \simeq -36$  to  $-30$  MeV, which is compatible with a reported  ${}^4n$  resonance region in Ref. [8], gives rise to the appearance of bound  $J = 2^-$  and  $J = 1^-$  states in  ${}^4\text{H}$ ,  ${}^4\text{He}(T = 1)$  and  ${}^4\text{Li}$  nuclei. Unlike observed in the collision experiments, these states become stable with respect to the  ${}^3\text{H}({}^3\text{He}) + N$  decay channels. This means that the present phenomenological  $W_1(T = 3/2)$  is too attractive to reproduce low-lying states of  ${}^4\text{H}$ ,  ${}^4\text{He}(T = 1)$  and  ${}^4\text{Li}$ .

In contrast, it is interesting to see the energy of  $4n$  system when we have just unbound states for  ${}^4\text{H}$ ,  ${}^4\text{He}(T = 1)$  and  ${}^4\text{Li}$  in Fig. 6a. Use of  $W_1(T = 3/2) = -19$  MeV gives rise to an unbound state with  $J = 2^-$  in  ${}^4\text{H}$  with respect to disintegration into  ${}^3\text{H} + N$ . However, using this strength of  $W_1(T = 3/2)$ , we have already a very broad  ${}^4n$  resonant state at  $\text{Re}(E_{\text{res}}) = 6$  MeV with  $\Gamma = 7.5$  MeV, see Fig. 4a, which is inconsistent with the recent experimental claim [8] of a resonant  ${}^4n$ . Moreover the value of  $W_1(T = 3/2)$  that reproduces the observed broad resonance data for the  $2^-$  state in  ${}^4\text{H}$  should be much less attractive than  $-19$  MeV.

Results presented in Fig. 6a, however, give little insight to the properties of  ${}^4\text{H}$ , once it becomes a resonant state for  $W_1(T = 3/2) > -19$  MeV. Moreover it is well known [52], that for broad resonances the structure given by the S-matrix poles may be different from that provided by an R-matrix analysis. Therefore, it makes much more sense to perform direct calculations of the measurable  ${}^3\text{H}+n$  data, namely scattering cross sections. We display in Fig. 7 the  ${}^3\text{H}+n$  total cross section calculated for a value of  $W_1(T = 3/2) = -10$  MeV. This cross section is clearly dominated by pronounced

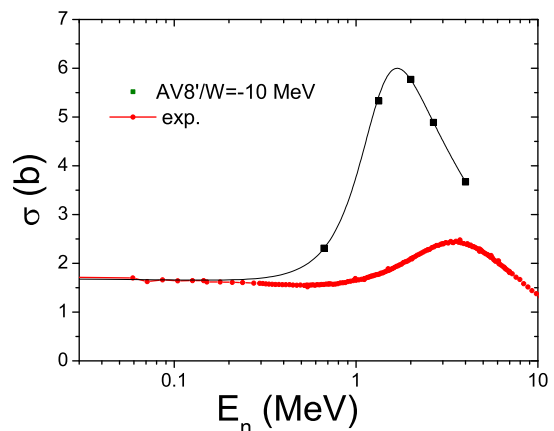


FIG. 7: (Color online) The calculated total cross section of  ${}^3\text{H}+n$  represented by thin black solid line using  $W_1(T=3/2)=-10$  MeV. The experimental data [53] are illustrated by the red thick solid line.

negative-parity resonances in the  ${}^4\text{H}$  system. These resonances contribute too much in the total cross section, resulting in the appearance of a narrow peak shifted significantly to the lower-energy side. Furthermore, in order to reproduce the shape of the experimental  ${}^3\text{H}+n$  cross section, a very weak 3NF is required in the isospin  $T = 3/2$  channel. From this fact, we conclude that even a  $W_1(T = 3/2) = -10$  MeV value renders the 3NF to be excessively attractive.

In conclusion, as far as we can maintain the consistency with the observed low-lying energy properties of the  ${}^4\text{H}$ ,  ${}^4\text{He}$  ( $T = 1$ ) and  ${}^4\text{Li}$  nuclei, it is difficult to produce an observable  ${}^4n$  resonant state.

#### D. $3n$ resonances

Finally, in Fig. 8, we show the calculated resonance poles of the trineutron  ${}^3n$  system for the lowest-lying negative- and positive-parity states ( $J = 3/2^-, 1/2^-$  and  $1/2^+$ ). The strength  $W_1(T = 3/2)$  is increased so that there appears a broad resonance with  $\text{Im}(E_{\text{res.}}) \approx -\text{Re}(E_{\text{res.}})$ .

Although it is reasonable to have the negative-parity states much lower than the positive-parity ones from the viewpoint of a naive  $3n$  shell-model configuration, we have to impose a value of  $W_1(T = 3/2)$ , a few times stronger than in the  ${}^4n$  system to bind  ${}^3n$ .

For  $W_1(T = 3/2) = -40$  MeV, the most favorable  ${}^3n$  resonance with  $J = 3/2^-$  is located at  $\text{Re}(E_{\text{res.}}) \sim 4$  MeV with  $\Gamma \sim 8$  MeV as seen in Fig. 8, whereas the  $J = 0^+$   ${}^4n$  state is still bound at  $E = -4.5$  MeV (cf. Fig. 4b).

On the other hand the  ${}^3n$  is a much more repulsive system than the  ${}^4n$  one, which benefits from the presence of two al-

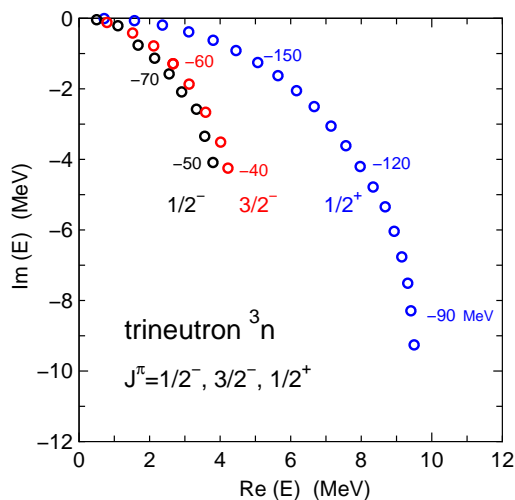


FIG. 8: (Color online) Trineutron  ${}^3n$  resonance trajectories for  $J = 3/2^-, 1/2^-$  and  $1/2^+$  states. The circles correspond to resonance positions for  $W_1(T = 3/2)$  from  $-75$  to  $-40$  MeV for  $J = 3/2^-$ , from  $-90$  to  $-50$  MeV for  $J = 1/2^-$  and from  $-180$  to  $-85$  MeV for  $J = 1/2^+$  in step of 5 MeV.

most bound bosonic dineutron pairs. On the other hand  ${}^4n$  is much more sensitive to the 3NF than  ${}^3n$ , as four neutrons involve four 3NF interactions compared to single one present in three neutrons. From this result one can expect that if the 3NF contribution turns out to be important in the  ${}^4n$  system rendering it resonant, other multineutron systems with  $A > 4$  (in particular  ${}^6n$  and  ${}^8n$ ) would display even more prominent resonant structures than  ${}^4n$ .

## V. CONCLUSIONS

Motivated by the recent experimental claim regarding the possible existence of observable tetra-neutron  ${}^4n$  [7, 8] states, we have investigated the possibility that the  $4n$  system exhibits a near-threshold bound or narrow resonant state compatible with the reported data.

When studying the tetra-neutron sensitivity to the ingredients of the nuclear interaction, we have concluded that this system is not very sensitive to “experimentally allowed” modifications in  $NN$  interaction. The most natural way to enhance a tetra-neutron system near the threshold is through an additional attractive isospin  $T = 3/2$  term in the three-body force. We have examined the consistency of the nuclear Hamiltonian modifications, required to produce observable tetra-neutron states, with other four-nucleon observables, like the low-lying  $T = 1$  states in  ${}^4\text{H}$ ,  ${}^4\text{He}$  and  ${}^4\text{Li}$ .

This study has been based on the  $4N$  Hamiltonian considered in Ref. [42] built from the AV8' version of the  $NN$  potential produced by the Argonne group and supplemented with a phenomenological  $3N$  force including both  $T = 1/2$  and  $T = 3/2$  terms. The  $T = 1/2$  term was adjusted [42] to properly reproduce the binding energies of the  ${}^3\text{H}$  and  ${}^3\text{He}$  ground states and the  ${}^4\text{He}$  ground and first  $0^+$  excited states as well as the transition form factor  ${}^4\text{He}(e, e'){}^4\text{He}(0_2^+)$ . In order to check the model independence of our results we have also considered the INOY potential which markedly differs from the preceding ones in its non local character that incorporates the  $T = 1/2$  3NF. Despite of these differences the results were very close to each other.

The  $T = 3/2$  component added in the present work, has the same functional form as the  $T = 1/2$  one and contains one single free parameter – the strength of its attractive part – which was adjusted in order to generate a  $4n$  bound or resonant states. The validity of the strength of  $T = 3/2$  parameter found in this way, was investigated by calculating the  $T = 1$ ,  $J^\pi = 2^-$  and  $1^-$  states of  ${}^4\text{H}$ ,  ${}^4\text{He}$  and  ${}^4\text{Li}$  as well as the total cross section of the  ${}^3\text{H}+n$  scattering, which turned out to be very sensitive to the  $T = 3/2$   $3N$  force.

The *ab initio* scattering solutions of the  $4n$  Hamiltonian were obtained using the appropriate boundary condition of a four-body resonance provided by the complex scaling method. The Gaussian expansion method and the Faddeev-Yakubovsky formalisms were used for solving the  $A = 4$  problem. The two methods provide accurate results and agreed with each other within at least two significant digits, both for the resonant as well as for the bound states.

In order to produce resonant tetraneutron states which were situated in the complex energy plane close to the physical axis, and, thus may have an observable impact, we were obliged to introduce strong modifications in the  $T = 3/2$   $3N$  force. These modifications were however found to be inconsistent with other well established nuclear properties and low energy scattering data. This result is in line with our previous study of the tetraneutron system[17].

In conclusion, we were not able to validate the recent observation of a  ${}^4n$  signal [7, 8] as related to the existence of resonant  $4n$  states.

Further experimental studies of the tetraneutron system are planned in the near future at RIKEN [54–56] to confirm the finding of [7, 8] with higher statistic. If this would be the case it will constitute a real challenge for theoretical interpretation.

Another possibility could be that the low-energy  ${}^4n$  signal is a result of some unknown dynamical phenomena, which is not directly related to the existence of  $S$ -matrix (resonance) poles in the  ${}^4n$  system. In this respect it is worth mentioning that, in the framework of the scattering theory, there exist

other possibilities to generate sharp structures in a reaction cross section without any presence of  $S$ -matrix pole singularities [57]. Such phenomena have not yet been established in any physical system.

### Acknowledgments

The authors thank Dr. S. Shimoura, Dr. K. Kisamori, Dr. H. Sakai, Dr. F. M. Marques, Dr. V. Lapoux for valuable discussion. This work was partially performed in the "Espace de Structure Nucléaire Théorique" (ESNT, <http://esnt.cea.fr>) at CEA from which the authors acknowledge support. The numerical calculations were performed on the HITACHI SR16000 at KEK, YITP in Kyoto University and HPC resources of TGCC under the allocation 2015-x2015056006 made by GENCI. We thank the staff members of these computer centers for their constant help. This work was partly supported by RIKEN iTHES Project .

- 
- [1] A.A. Oglobin and Y.E. Penionzhkevich, in *Treatise on Heavy-Ion Science, Nuclei Far From Stability*, Vol. 8, ed. by D.A. Bromley (Plenum Press, New York, 1989) p. 261.
- [2] D. R. Tilley, H. R. Weller and G. M. Hale, *Nucl. Phys. A* **541**, 1 (1992).
- [3] F. M. Marques, Lecture given at "Ecole Joliot-Curie de Physique Nucleaire", Maubuisson (France) Sep. 2002.
- [4] F. M. Marques, *et al.*, *Phys. Rev. C* **65**, 044006 (2002).
- [5] L.V. Chulkov *et al.*, *Nucl. Phys. A* **759**, 43 (2005)
- [6] F. M. Marques, N. A. Orr, H. Al Falou, G. Normand, N. M. Clarke, arXiv nucl-ex/0504009
- [7] K. Kisamori, Ph.D. thesis (Univ. of Tokyo, 2015).
- [8] K. Kisamori *et al.*, *Phys. Rev. Lett.* **116**, 052501 (2016).
- [9] S. Fortier *et al.*, *Nucl. Phys. A* **805**, 320 (2008).
- [10] J.J. Bevelacqua, *Nucl Phys. A* **431**, 414 (1980).
- [11] A.M. Badalyan, T.I. Belova, N.B. Konyuhova, V.D. Efros, *Sov. J. Nucl. Phys.* **41**, 926 (1985).
- [12] A.M. Gorbатов *et al.*, *Yad. Fiz.* **50**, 347 (1989).
- [13] S.A. Sofianos, S.A. Rakityansky, and G.P. Vermaak, *J. Phys. G* **23**, 1619 (1997).
- [14] N. K. Timofeyuk, *J. Phys. G* **29**, L9 (2003).
- [15] S. C. Pieper, *Phys. Rev. Lett.* **90**, 252501 (2003).
- [16] R. Lazauskas, Ph.D., Univ. J. Fourier, Grenoble (2003); <http://tel.ccsd.cnrs.fr/documents/archives0/00/00/41/78/>.
- [17] R. Lazauskas and J. Carbonell, *Phys. Rev. C* **72**, 034003 (2005).
- [18] R. Lazauskas and J. Carbonell, *Phys. Rev. C* **71**, 044004 (2005).
- [19] R. B. Wiringa, V. G. J. Stoks and R. Schiavilla, *Phys. Rev. C* **51**, 38 (1995)
- [20] S. C. Pieper, V. R. Pandharipande, R. B. Wiringa, and J. Carlson, *Phys. Rev. C* **64**, 014001 (2001).
- [21] V.I. Kukulin, V.M. Krasnopol'sky and J. Horacek: *Theory of Resonances, Principles and Applications* (Kluwer 1989).
- [22] O.A. Yakubovsky, *Sov. J. Nucl. Phys.* **5**, 937 (1967).
- [23] V.G.J. Stoks, R.A.M. Klomp, C.P.F. Terheggen, J.J. de Swart, *Phys. Rev. C* **49**, 2950 (1994).
- [24] R. Machleidt, *Phys. Rev. C* **63**, 024001 (2001).
- [25] H. Witala and W. Gloeckle, *Phys.Rev. C* **85**, 064003 (2012).
- [26] E. Epelbaum *et al.*, *Phys. Rev Lett.* **86**, 4787 (2001)
- [27] M. H. Wood *et al.*, *Phys.Rev.* **C65**, 034002 (2002).
- [28] P. Doleschall, *Phys. Rev. C* **69**, 054001 (2004).
- [29] J. Aguilar, and J.M. Combes, *Commun. Math. Phys.* **22**, 269 (1971).
- [30] E. Balslev, and J.M. Combes, *Commun. Math. Phys.* **22**, 280 (1971).
- [31] B. Simon, *Commun. Math. Phys.* **27**, 1 (1972).
- [32] Y. K. Ho, *Phys. Rep.* **99**, 1 (1983).
- [33] N. Moiseyev, *Phys. Rep.* **302**, 211 (1998).
- [34] M. Kamimura, *Phys. Rev. A* **38**, 621 (1988).
- [35] H. Kameyama, M. Kamimura, and Y. Fukushima, *Phys. Rev. C* **40**, 974 (1989).
- [36] E. Hiyama, Y. Kino, and M. Kamimura, *Prog. Part. Nucl. Phys.* **51**, 223 (2003).
- [37] E. Hiyama, *Few-Body Systems* **53**, 189 (2012).
- [38] E. Hiyama, *Prog. Theor. Exp. Phys.* **2012**, 01A204 (2012).
- [39] E. Hiyama and M. Kamimura, *Phys. Rev. A*, **85**, 022502 (2012); *ibid.* **85**, 062505 (2012); *ibid.* **90**, 052514 (2014).
- [40] B. S. Pudliner, V. R. Pandharipande, J. Carlson, S. C. Pieper, and R. B. Wiringa, *Phys. Rev. C* **56**, 1720 (1997).
- [41] H. Kamada, A. Nogga, W. Glöckle, E. Hiyama, M. Kamimura, K. Varga, Y. Suzuki, M. Viviani, A. Kievsky, S. Rosati, J. Carlson, S. C. Pieper, R. B. Wiringa, P. Navratil, B. R. Barrett, N. Barnea, W. Leidemann, and G. Orlandini, *Phys. Rev. C* **64**, 044001 (2001).
- [42] E. Hiyama, B.F. Gibson, and M. Kamimura, *Phys. Rev. C* **70** 031001(R) (2004).
- [43] S. Aoyama, T. Myo, K. Kato, and K. Ikeda, *Prog. Theor. Phys.* **116**, 1 (2006).
- [44] T. Myo, Y. Kikuchi, H. Masui, and K. Kato, *Prog. Part. Nucl. Phys.* **79**, 1 (2014).
- [45] J. Carbonell, A. Deltuva, A.C. Fonseca, and R. Lazauskas, *Prog. Part. Nucl. Phys.* **74**, 55 (2014).
- [46] S. Ohtsubo, Y. Fukushima, M. Kamimura, and E. Hiyama, *Prog. Theor. Exp. Phys.* **2013**, 073D02 (2013).
- [47] E. Hiyama, S. Ohnishi, M. Kamimura, and Y. Yamamoto, *Nucl. Phys. A* **908**, 29 (2013).
- [48] E. Hiyama, M. Isaka, M. Kamimura, T. Myo, and T. Motoba,

- Phys. Rev. C **91**, 054316 (2015).
- [49] G.L. Payne and B.F. Gibson, Few-Body Syst. **14**, 117 (1993).
- [50] D. Baye, Phys. Rep. **565** (2015) 1.
- [51] K. Hebeler, H. Krebs, E. Epelbaum, J. Golak, and R. Skibinski, Phys. Rev. C **91**, 044001 (2015).
- [52] D.R. Tilley, H.R. Weller, and G.M. Hale, Nucl. Phys. A **541**, 1 (1992).
- [53] T.W. Phillips and B.L. Berman, Phys. Rev. C **22**, 384 (1980).
- [54] S. Shimoura *et al.*, RIKEN-RIBF proposal on ' Tetra-neutron resonance produced by exothermic double-charge exchange reaction', NP1512-SHARAQ10.
- [55] K. Kisamori *et al.*, RIKEN-RIBF proposal on ' Many-neutron systems:search for superheavy  ${}^7\text{H}$  and its tetraneutron decay', NP-1512-SAMURAI34
- [56] S. Paschalis, S. Shimoura *et al.*, RIBF Experimental Proposal NP1406-SAMURAI19.
- [57] G. Calucci, and C. Ghirardi, Phys. Rev. **169**, 1339 (1968).